Further insight into the involvement of PII1 in starch granule initiation in Arabidopsis leaf chloroplasts

Camille Vandromme[1], Corentin Spriet[1,2] , Jean-Luc Putaux[3] , David Dauvillée[1] , Adeline Courseaux[1] , Christophe D'Hulst[1] and Fabrice Wattebled[1]

[1]Univ. Lille, CNRS, UMR 8576 – UGSF – Unité de Glycobiologie Structurale et Fonctionnelle, F-59000 Lille, France; [2]Univ. Lille, CNRS, Inserm, CHU Lille, Institut Pasteur de Lille,

US 41 – UAR 2014 – PLBS, F-59000 Lille, France; [3]Univ. Grenoble Alpes, CNRS, CERMAV, F-38000 Grenoble, France

Summary

Author for correspondence:
Fabrice Wattebled
Email: *fabrice.wattebled@univ-lille.fr*

- The control of starch granule initiation in plant leaves is a complex process that requires active enzymes like Starch Synthase 4 and 3 (SS4 or SS3) and several noncatalytic proteins such as Protein Involved in starch Initiation 1 (PII1). In Arabidopsis leaves, SS4 is the main enzyme that control starch granule initiation, but in its absence, SS3 partly fulfills this function. How these proteins collectively act to control the initiation of starch granules remains elusive. PII1 and SS4 physically interact, and PII1 is required for SS4 to be fully active. However, Arabidopsis mutants lacking SS4 or PII1 still accumulate starch granules.
- Combining *pii1* KO mutation with either *ss3* or *ss4* KO mutations provide new insights of how the remaining starch granules are synthesized.
- The *ss3 pii1* line still accumulates starch, while the phenotype of *ss4 pii1* is stronger than that of *ss4*.
- Our results indicate first that SS4 initiates starch granule synthesis in the absence of PII1 albeit being limited to one large lenticular granule per plastid. Second, that if in the absence of SS4, SS3 is able to initiate starch granules with low efficiency, this ability is further reduced with the additional absence of PII1.

Introduction

Starch is a storage polymer that is synthesized in the plastids of photosynthetic organisms. It is composed of two structurally distinct α-linked glucans: amylose and amylopectin that are intricately combined in the form of dense, cold-water insoluble granules. Starch granule morphology and size are variable between species (Streb & Zeeman, 2012). In wild-type Arabidopsis leaves, starch granules, that accumulate between thylakoids, have a smooth, more, or less regular, lenticular form. The average number of granules per plastid also fluctuates. In photosynthetic plastids of a source organ, several granules are generally synthesized. For instance, Arabidopsis leaf chloroplasts generally contain 5–7 starch granules (Crumpton-Taylor *et al.*, 2012). The number of granules in nonphotosynthetic plastids is lower, being, in some species, reduced to only one, like in potato tubers (Kram *et al.*, 1993).

Currently, the process underlying the initiation of a new starch granule and the control of the number of granules per plastid has gained a lot of attention since it impacts the granule size and shape, parameters that strongly influence starch transformation and the quality of starch-based end products (Jobling, 2004; Singh *et al.*, 2007; Guo *et al.*, 2014; Tao *et al.*, 2016). Over the past few years, numerous proteins have been described being

involved in the priming and hence the control of starch granule formation. Most of these proteins are noncatalytic such as Protein Involved in starch Initiation 1 (PII1, also called MRC for Myosin-Resembling Chloroplast protein), Mar-binding Filament-like Protein 1 (MFP1), Protein Targeting to Starch 2 and 3 (PTST2 and PTST3) and Starch synthase 5 (SS5; Seung *et al.*, 2017; Seung *et al.*, 2018; Vandromme *et al.*, 2019; Abt *et al.*, 2020). Other proteins are catalytically active such as SS4. The inactivation of SS4 activity in *Arabidopsis* leaves leads to a grossly modified pattern of starch granule morphology (rounded rather than lenticular) and number (0–1 granule per chloroplast rather than 5–7) suggesting a preeminent function of this enzyme in the control of starch granule formation and initiation (Roldán *et al.*, 2007; Crumpton-Taylor *et al.*, 2013; Bürgy *et al.*, 2021). Interestingly, starch granule initiation is tightly controlled and occurs in specific regions of the chloroplast located between thylakoid membranes (Bürgy *et al.*, 2021). How this happens remains unclear but is likely related to the control of SS4 distribution within the plastid. This distribution could be driven by plastidial proteins directly or indirectly interacting with SS4. This is for instance the case of the thylakoid-localized fibrillins and the noncatalytic MFP1 protein that were both reported to physically interact with SS4 (Gámez-Arjona *et al.*, 2014; Seung *et al.*, 2018). In addition, it was recently demonstrated that

PTST2 and PTST3 are plastidial proteins that can bind glucans and that PTST2 interact with SS4 (Seung *et al.*, 2017). It was then suggested that both PTST2 and PTST3 could provide the priming substrate required by SS4 to initiate the synthesis of starch granules in specific plastidial regions (Seung *et al.*, 2017).

Starch synthase 4 is composed of two domains. The C-terminal moiety of the protein contains the catalytic Glycosyl transferase 5 (GT5) domain conserved among the starch synthases and was shown to control the starch granule number in Arabidopsis chloroplasts (Lu *et al.*, 2018). The N-terminal moiety of SS4, which contains several coiled-coil regions, controls both the proper localization of the protein within the stroma and the shape of the granule (Raynaud *et al.*, 2016; Lu *et al.*, 2018).

In a previous study, using double-hybrid and BiFC methods, we identified PII1 as a protein that physically interacts with SS4. Protein Involved in starch Initiation 1 has no known activity, and no specific function can be determined through its primary structure. In *pii1* KO mutants, we found a reduction in the starch granule number per chloroplast (one granule per plastid on average). However, contrary to what happens in *ss4* mutants, these granules remain lenticular such as in the wild-type. Thus, we hypothesized that PII1 is required for the proper catalytic activity of SS4 but not for the control of the lenticular growth of starch granules by SS4 (Vandromme *et al.*, 2019).

Moreover, other works revealed that in the absence of SS4, the synthesis of the residual starch granules in the Arabidopsis chloroplasts depends on the presence of SS3, another isoform of starch synthase. Indeed, starch content drops to almost zero in the *ss3 ss4* double mutant (Szydlowski *et al.*, 2009; Crumpton-Taylor *et al.*, 2013).

From these results, several issues remain to be elucidated. The first was to determine which starch synthase (SS3 or SS4) is responsible for starch granule initiation in *pii1*. Indeed, it is still possible that SS4 activity is altered and not completely inactivated in *pii1* leading to the formation of one granule per chloroplast. Alternatively, it is also possible that in *pii1*, the priming activity of SS4 is totally inactivated while that of SS3 is stimulated because of the lack of PII1 (the N-terminal part of SS4 being still able to drive the lenticular growth of the granule). Both hypotheses could explain why the phenotype of *pii1* is less severe than that of *ss4*. If SS3 primes starch granules synthesis in the *pii1* mutant background, the *ss3 pii1* double mutant, such as the *ss3 ss4* double mutant, should be starch-free. If not, *ss3 pii1* should resemble the phenotype of *pii1*. The second issue was to determine whether PII1 is also involved in the mechanism of starch initiation fulfilled by SS3 in the absence of SS4. Thus, removing PII1 in addition to that of SS4 would give different phenotypes whether PII1 assists or not SS3 for its priming activity. To answer these two questions, we generated and analyzed both *ss3 pii1* and *ss4 pii1* mutants, respectively. The results presented here show that the *ss3 pii1* mutant is not free of starch but, on the contrary, contains granules with distorted shapes, while the *ss4 pii1* mutant accumulates less starch than the *ss4* single mutant. The results are discussed and provide further insight into the function of PII1 in the control of starch granule synthesis.

Materials and Methods

Plant material and growth conditions

Arabidopsis thaliana Wassilewskija (Ws) and Columbia (Col-0) lines can be ordered from SiGnAL (Alonso *et al.*, 2003). All mutant alleles used in this study have been described previously (Zhang *et al.*, 2005; Roldán *et al.*, 2007; Szydlowski *et al.*, 2009, 2011; Vandromme *et al.*, 2019). Germplasm references and position of the different mutations are described in Fig. 1. Crosses and selection of the double mutant lines were performed from plants grown in the glasshouse. Regulation system was set to obtain 16 h : 8 h, light (150 µmol photon $m^{-2} s^{-1}$) : dark photoperiod with c. 23°C : 20°C, day : night. For plant growth analysis or starch extraction, plants were grown in a growth chamber with 16 h : 8 h, light (120 µmol photon $m^{-2} s^{-1}$) : dark photoperiod, 23°C : 20°C. In all cases, 3 d before being sown, seeds were incubated at 4°C in 0.1% phytagel solution.

Chloroplast observation and determination of starch priming efficiency

Leaves of 2-wk-old plants were harvested at the end of the light phase. Sections of proximal or distal part of the leaves were transferred in 1 ml of fixating solution (4% (w/v) paraformaldehyde, 4% (w/v) sucrose, and 1× PBS at pH 7.3). Samples were placed under vacuum during 6 h and stored at 4°C. Leaf samples were placed between microscope slide and coverslip and observed under A1 Nikon confocal microscope (Nikon Instruments Europe B.V., Amstelveen, the Netherlands) with a Plan Apo ×60 Oil (NA = 1.4) objective. Autofluorescence was acquired with $\lambda_{ex} = 488$ nm–$\lambda_{em} = 500$–550 nm and $\lambda_{ex} = 561$ nm–$\lambda_{em} = 580$–620 nm. The observation and determination of starch granule number per chloroplast were carried out through live Z scanning of the whole chloroplasts to avoid bias due to out-of-focus starch granules. Granules were counted during the acquisition by two researchers, and a representative image was acquired. After acquisition, we used Fiji (Schindelin *et al.*, 2012) to apply: (1) a median filter with a 'radius' of 0.5; (2) a high accuracy Contrast Limited Adaptive Histogram Equalization (CLAHE (Zuiderveld, 1994)) with a maximum slope of 2.5; and (3) a brightness equalization between images.

Starch extraction, purification, and quantification

The leaves of 3-wk-old plants were harvested at the end of the light or dark phases and immediately frozen in liquid nitrogen. Depending on the purpose, quantification, or purification, two different protocols were applied.

For starch quantification, leaf samples were weighted and 0.3–0.5 g were disrupted using a polytron blender in 5 ml of 1 M perchloric acid. Samples were centrifuged at 4500 *g* for 10 min at 4°C. The pellet containing starch was rinsed three times with sterile deionized water and stored at 4°C in 1 ml of 20% ethanol.

The starch amount was determined using Enzytec™ starch kit. 30 µl of different sample dilutions was boiled during 10 min;
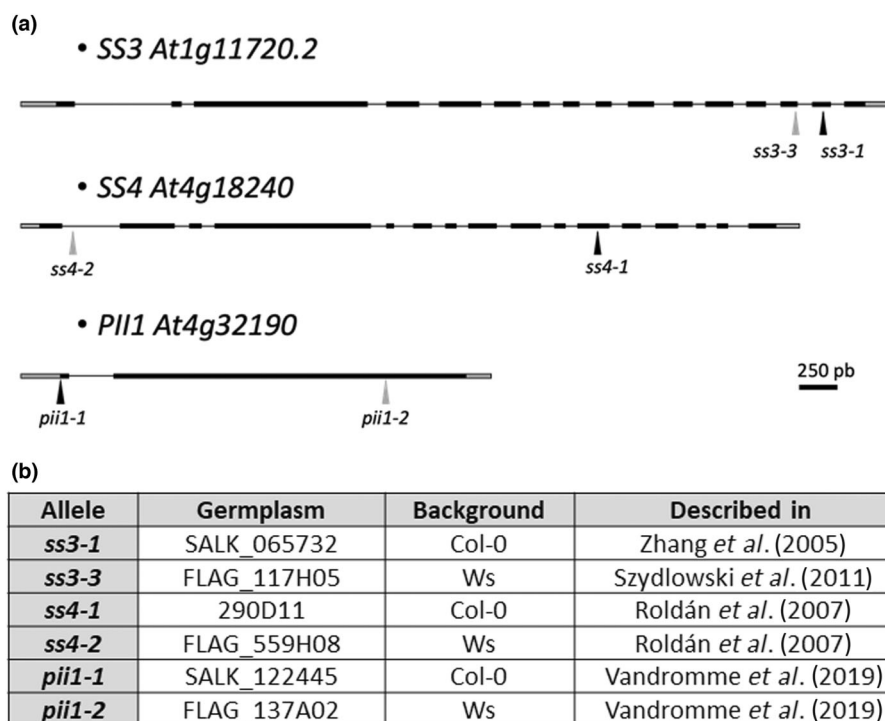
Fig. 1 Identification of the different alleles. (a) Structure of Arabidopsis Starch synthase 3 (*SS3*), *SS4*, and Protein Involved in starch Initiation 1 (*PII1*) genes. 3′ and 5′ UTR are indicated by gray boxes while introns and exons are represented by black lines and boxes respectively. The locations of T-DNA insertions are indicated by black triangles (insertion in Col-O genetic background) or gray triangles (insertion in Ws genetic background). (b) Summary of the different alleles used in this work, germplasm identification, genetic background, and references where the mutant lines are described.

Allele	Germplasm	Background	Described in
ss3-1	SALK_065732	Col-0	Zhang *et al.* (2005)
ss3-3	FLAG_117H05	Ws	Szydlowski *et al.* (2011)
ss4-1	290D11	Col-0	Roldán *et al.* (2007)
ss4-2	FLAG_559H08	Ws	Roldán *et al.* (2007)
pii1-1	SALK_122445	Col-0	Vandromme *et al.* (2019)
pii1-2	FLAG_137A02	Ws	Vandromme *et al.* (2019)

60 µl of amyloglucosidase (14 U ml^{-1}) was added. The medium was incubated for 45 min at 58°C and centrifuged for 10 min at 10 000 g and 4°C. 30 µl of digested starch was transferred in a 96-well plate. The following steps were carried out according to the manufacturer's instruction with the provided buffer and enzymes. 100 µl of buffer 1 and 100 µl of deionized water were added. The initial absorbance was recorded at 340 nm. 2 µl of enzyme mix were used and the final absorbance at 340 nm was recorded to complete the assay. Four independent cultures were grown, and for each culture, three biological samples were harvested per genotype. We then normalized the values by calculating, for each culture, the average obtained for the wild-type reference. We established this value as 100% and expressed the amount of starch accumulated by the different genotype as a percentage of the wild-type amount. We then calculated a mean and a standard error from the 12 values obtained for each of the genotypes. A two-tailed t-test with unequal variance was applied using an EXCEL function. Statistically meaningful differences were indicated by either one asterisk ($P < 0.05$) or two asterisks ($P < 0.001$).

A different protocol was used when purified starch was needed for microscopy analysis, starch fractionation, or determination of chain length distribution (CLD). Several grams of leaves were disrupted using a Polytron blender in a buffer composed of 100 mM MOPS, pH 7.2, 5 mM EDTA, and 10% (v/v) ethylene glycol. The homogenate was filtered through two layers of Miracloth (Calbiochem; EMD Millipore Corp., Billerica, MA, USA). The filtrate was centrifuged at 4000 g during 10 min at 4°C. The supernatant was discarded, and the pellet was resuspended in 2 ml of 90% (v/v) Percoll. The sample was centrifuged for 45 min at 10 000 g and 4°C. The starch pellet was washed several times with 2 ml of sterile deionized water and stored in 1 ml of 20% ethanol.

Scanning electron microscopy and starch granule size distribution

The procedure was identical to the one described in Vandromme *et al.* (2019). Aqueous suspensions of purified starch granules were dropped on a piece of glow-discharged copper tape. When dried, samples were coated with Au/Pd and secondary electron images were recorded with a FEI Quanta 250 scanning electron microscope equipped with a field emission gun and operating at 2 kV. The starch granule size was determined from the scanning electron microscopy (SEM) images using FIJI software. The major axis of 300 granules was measured, and the average value was calculated.

Starch fractionation and determination of the amylose content

To evaluate the proportion of amylose in starch granules, two different methods were applied. First, we fractionated starch by size exclusion chromatography to separate amylopectin and amylose. 1.8 mg of starch was dispersed by boiling for 10 min in 200 µl of 100% dimethylsulfoxide (DMSO). The glucans were then precipitated by the addition of 800 µl of 100% ethanol and stored during several hours at −20°C. The samples were centrifuged at 10 000 g during 10 min at 4°C. The pellet was air-dried and solubilized in 300 µl of 10 mM NaOH. The sample was loaded at the top of a column (0.5 i.d. × 65 cm) filled with Sepharose CL-2B matrix and equilibrated with 10 mM NaOH. The flow

rate was set at $12 \, \text{ml h}^{-1}$. Fractions of 300 µl were collected. 80 µl of each fraction was mixed with 20 µl of a solution made of I_2 (0.1% w/v) and KI (1% w/v). The presence of glucans was detected by spectrophotometry analysis. Fractions containing amylopectin or amylose were pooled and the amount of polysaccharides was determined by enzymatic assay (as previously described).

The second method that was applied is described in Helle *et al.* (2019) and used the Megazyme (Wicklow, Ireland) kit amylose/amylopectin assay (K-Amyl). 1.5 mg of starch was gelatinized in 200 µl of 100% DMSO at 100°C during 15 min. Polysaccharides were precipitated by the addition of 800 µl of 100% ethanol. The sample was centrifuged for 5 min at 2000 *g*. The pellet was suspended in 120 µl of 100% DMSO and heated at 100°C during 15 min. Amylopectin was precipitated following the manufacturer's instructions using concanavalin A (ConA). The sample containing the polysaccharides was gently mixed with 1.5 ml of ConA solvent (this 1.5 ml containing amylose and amylopectin is designed as Solution A). 300 µl of this solution was mixed with 150 µl of ConA in order to precipitate the amylopectin fraction during 1 h of incubation at room temperature. A 10 min centrifugation at 14 000 *g* allowed the separation of amylose (in the supernatant) and amylopectin (in the pellet). 300 µl of the supernatant was mixed with 300 µl of 100 mM sodium acetate buffer (pH 4.5) and heated at 100°C during 5 min. This allowed ConA to be denatured. Then, 800 µl of sodium acetate buffer was added to 100 µl of solution A. 20 µl of the amylose fraction and 20 µl of diluted solution A were digested with 20 µl of solution 2 (provided by manufacturer and containing amyloglucosidase and α-amylase) during 30 min at 40°C. 40 µl of the digested samples was transferred into 96-well plates, and 160 µl of GOPOD reagent was added to each well. After 20 min of incubation at 40°C, the absorbance was measured at 510 nm using a spectrophotometer. The amylose percentage was calculated according to the manufacturer's instructions.

Polysaccharide chain length distribution

The amylopectin CLD was determined using fluorescence-assisted capillary electrophoresis as described in Helle *et al.* (2019). 1.8 mg of starch was boiled in 250 µl of sterile ultrapure water during 10 min. 250 µl of sodium acetate 110 mM pH 3.5; 20 units of isoamylase (*Pseudomonas* sp. from Megazyme); and 1 unit of pullulanase (from Sigma-Aldrich E2412) were added. Samples were incubated overnight at 42°C. Proteins were eliminated by boiling the samples during 10 min before centrifugation (15 000 *g* for 10 min). The glucans-containing supernatants were desalted using a Carbograph column (Grace™ Alltech™, Extract-Clean™) and lyophilized. The glucans were solubilized in 2 µl of sodium cyanoborohydride in tetrahydrofuran and 2 µl of 0.2 M 8-aminopyrene-1,3,6-trisulfonic trisodium salt (APTS) in 15% acetic acid (v/v). The derivatization reaction occurred during overnight incubation at 42°C. 46 µl of ultrapure water was added at the end of the reaction. 1 µl of the dilution was mixed with 49 µl of water before injection in a

Beckman Coulter PA800-plus Pharmaceutical Analysis System (Beckman Coulter, Brea, CA, USA). A silicon capillary column (inner diameter: 50 µm, outer diameter: 360 µm, and length: 60 cm) was filled with Beckman Coulter N-linked carbohydrate separation gel buffer diluted to the third with ultrapure water. The sample was injected during 15 s at 10 kV. Migration was performed at 10 kV during 1 h at 20°C. A 488 nm solid-state laser module and a laser-induced fluorescence detector were used to detect the glucans labeled with APTS.

X-ray diffraction

The sample preparation protocol was adapted to take into account the very small amount of starch granules available. To prevent any loss of material, the specimens were manipulated in the form of aqueous suspensions that were first concentrated by centrifugation. A small volume of the wet pellets (*c.* 4 µl) was pipetted and poured into 0.7-mm (outer diameter) glass capillaries. The capillaries were centrifuged again to concentrate the granules at the bottom, then flame-sealed. The pellets (in excess water) were X-rayed in transmission in a vacuum chamber using a Philips PW3830 generator operating at 30 kV and 20 mA (Ni-filtered CuKα radiation, λ = 0.1542 nm). Two-dimensional X-ray diffraction (XRD) patterns were recorded on Fujifilm imaging plates read with a Fujifilm BAS 1800-II bioimaging analyzer. Diffraction profiles were calculated as radial averages of the 2D patterns.

Additional materials and methods

Supporting Information Methods S1 describes the methods used for the selection of *ss3pii1* and *ss4pii1* lines, for the SDS-acrylamide gel electrophoresis and measurement of ADP-glucose concentration.

Results

Plant growth phenotype

We used already characterized *ss3*, *ss4*, and *pii1* mutants to combine mutations in either Ws or Col-0 ecotypes (Figs 1, S1; Table S1). Since the *pii1-1* mutation isolated in a Col-0 is leaky (Seung *et al.*, 2018), all the experiments described in this work were carried out in Ws genetic background. However, the main results obtained in the Ws ecotype were confirmed in the Col-0 background and are presented in Figs S2–S6. The plants were grown under 16 h : 8 h, light : dark cycles. The aboveground organs were collected at different time points and weighed. As already reported under these conditions, *ss3* and *pii1* single mutant behave like the wild-type (Zhang *et al.*, 2005, 2008; Vandromme *et al.*, 2019), while the *ss4* single mutant displayed a severe growth retardation (Roldán *et al.*, 2007). Combining *ss3* and *pii1* mutations led to reduced growth kinetics compared with the respective single mutants (Fig. 2a). Moreover, this double mutant displayed a slight delay (of *c.* 3 d) of the flowering time. Three-week-old Ws, *ss3*, and *pii1* plants have already developed

stems with flowers while *ss4*, *ss3 pii1*, and *ss4 pii1* plants have not (Fig. 3). Note that the growth kinetics of the *ss4 pii1* were similar to that of the *ss4* single mutant and that all plants bearing *ss4* mutation also have the pale green leaf phenotype described for this mutation (Roldán *et al.*, 2007; Fig. 2b).

Starch distribution in leaves

Leaf starch distribution was investigated by iodine-staining of 3-wk-old plants collected at the end of the light phase. In accordance with what has already been described, starch is homogeneously distributed in the leaves of wild-type, *ss3*, and *pii1* plants, while it is heterogeneously distributed in *ss4* (Fig. 3) being mostly present in the apex of the leaves. We show here that leaf starch distribution in the *ss3 pii1* line is similar to that of the wild-type,

ss3, and *pii1* lines, while that of the *ss4 pii1* double mutant resembles that of the *ss4* plants.

The number of starch granules in plastids was determined from confocal microscopy images of all lines analyzed in this work (Figs 4, S7; Table S2). Both proximal (close to the stem) and distal (apart of the stem) regions of the leaves were investigated and, depending on the genotypes, 90–250 chloroplasts were analyzed. As expected, most chloroplasts from wild-type and *ss3* plants contain 5–7 starch granules (rarely < 5 and > 6) with an average number between 5.32 ($\pm$0.08) and 5.72 ($\pm$0.11) whatever the considered leaf region (proximal or distal). In the *pii1* and *ss3 pii1* mutants, only one large starch granule was generally observed in the chloroplasts of both proximal and distal regions, with the average number of granules varying between 1.05 ($\pm$0.04) and 1.3 ($\pm$0.05). The *ss4 pii1* line behaves similarly

Fig. 2 Plant growth phenotypes. Arabidopsis plants were grown in a growth chamber under 16 h : 8 h, light : dark cycles. (a) The weight of aboveground organs is plotted against the number of days after germination. Two independent experiments were performed. For each experiment, all six genotypes are grown in the same chamber. Each value corresponds to the mean of three samplings ($\pm$SD). Wild-type (Ws) is depicted in blue lines, *ss3* in orange; *ss4* in gray; *pii1* in yellow; *ss3 pii1* in black; and *ss4 pii1* in green. Note that, on these graphs, *ss3* (*orange*) and wild-type (*blue*) profiles overlap and cannot be differentiated. *ss4* (in gray) and *ss4 pii1* (in green) are also almost identical. (b) Pictures of 3-wk-old plants. All pictures are at the same scale. Bar, 5 cm.
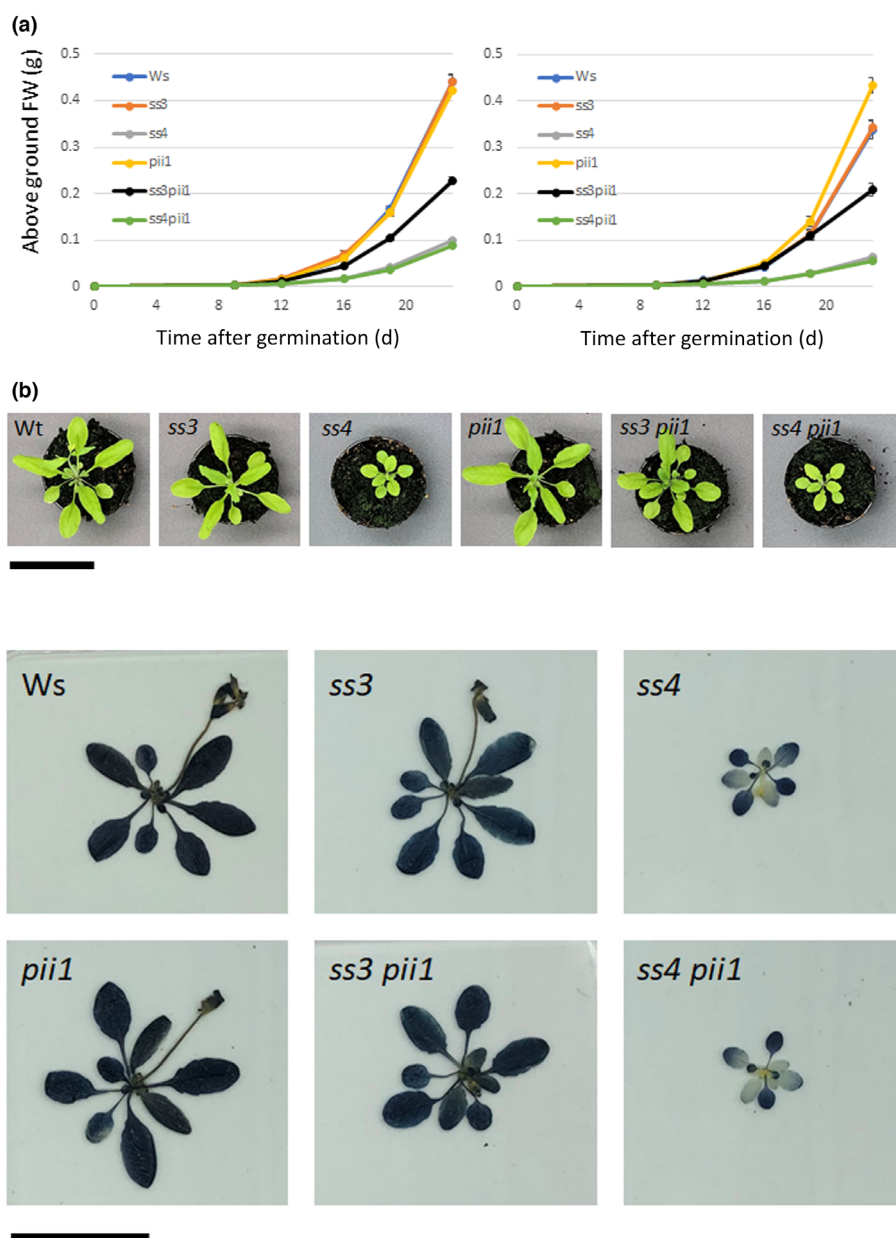

Fig. 3 Starch distribution in leaves. Arabidopsis plants were collected at the end of the light phase, 24 d after germination. Pigments were removed by incubation of plants in 80% ethanol at 80°C for 10 min. Plants were stained with iodine. Bar, 5 cm.
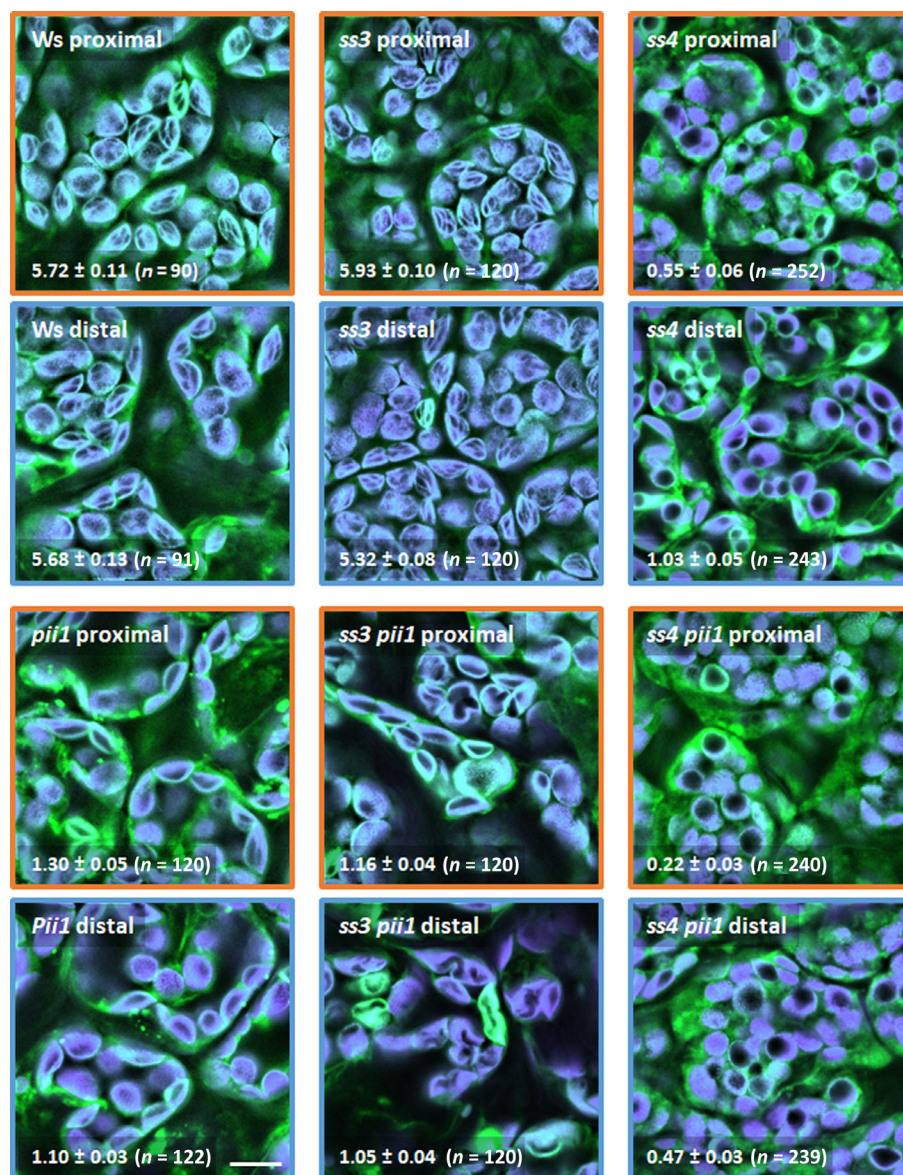
Fig. 4 Starch granule number in plastids. Leaves of 2-wk-old Arabidopsis plants were collected at the end of the day. Pieces of proximal (orange frame) and distal part (blue frame) of leaves were fixed in paraformaldehyde and analyzed by confocal microscopy. At the bottom of each picture, the average number of starch granules per chloroplast is indicated (±SE). Number of chloroplasts analyzed is indicated in brackets. Chlorophyll fluorescence in purple delimits the chloroplast volume; starch granules are black. Bar, 10 μm.

to the *ss4* mutant although its phenotype is exacerbated compared with the single mutant. Most plastids of the proximal region are starch-free in both *ss4* and *ss4 pii1*, the average number of granules being 0.55 (±0.06) in the *ss4* mutant and 0.22 (±0.03) in the *ss4 pii1* double mutant. In both *ss4* and *ss4 pii1* genotypes, the number of granules per plastid is increased in the distal region of the leaf in comparison with the proximal region (1.03 ± 0.05 and 0.47 ± 0.03 respectively). Regardless of the region observed, there is, in average less starch granules per chloroplast in *ss4 pii1* than in *ss4* (Table S2). The same approach was conducted for *ss4* and *ss4 pii1* mutants obtained in the Col-O genetic background and similar results were obtained (Fig. S4).

Shape and size of starch granules

The confocal microscopy observations described above suggested that the starch granules of *ss3 pii1* and *ss4 pii1* are modified both in size and shape compared with the wild-type. Indeed, the counting of the granules in the *ss3 pii1* double mutant was particularly challenging, even by varying the focus along the *z*-axis, because of the apparent grossly modified shape. Therefore, the starch granules were extracted and purified from these lines and observed by SEM (Fig. 5a). The *ss4 pii1* starch granules are spheroidal and very large compared with the smaller lenticular wild-type granules. This phenotype is quite similar to that already described for the *ss4* single mutants.

In the *ss3 pii1* mutant, starch granules are larger than those of the wild-type. Instead of the lenticular form (thin and round) usually observed for wild-type granules, the *ss3 pii1* granules have a considerably modified shape. Although they remain thin like the wild-type granules, they are much larger, like those of the *pii1* single mutant, but contrary to these latter, most of them do not remain flat. In the most extreme cases, the granules are significantly buckled (Fig. 5a,b for an enlarged view) giving them an
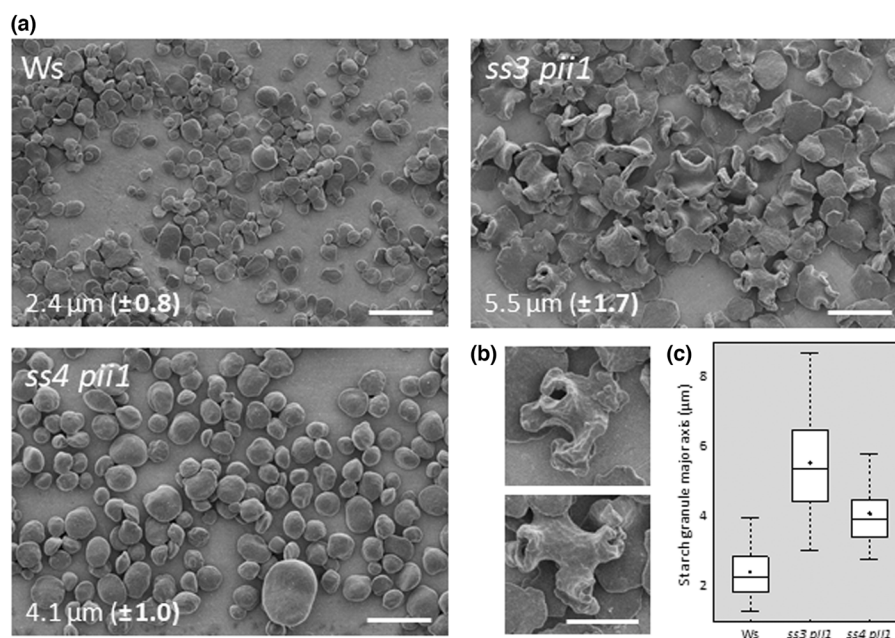
Fig. 5 Starch granule size and morphology. Starch granules were extracted at the end of the illuminated period from 3-wk-old Arabidopsis plants cultivated in 16 h : 8 h, light : dark photoperiods. (a) The purified starch granules were observed by scanning electron microscopy (SEM), and their major axis was measured using FIJI software. The average values (±SD), calculated from the measurement of 300 granules, are indicated. Bars, 10 μm. (b) Enlargement of *ss3pii1* starch granules selected from the image in (a), with marked alteration in their shapes. Bar, 5 μm. (c) For each genotype, the major axis of 300 starch granules was measured from SEM images using FIJI software. The solid line in the box corresponds to the median. The bottom and top of the boxes correspond respectively to the 25th and 75th percentiles. The dotted lines delimit the interval between the 5th and the 95th percentiles. The average value is indicated by a black dot.

irregular shape. This buckled phenotype is specific to the *ss3 pii1* mutant and was not described in the corresponding single mutants (Szydlowski *et al.*, 2011; Vandromme *et al.*, 2019).

The average size of the starch granules was estimated from the SEM images using the FIJI software. Three hundred starch granules were analyzed for each genotype and the major axis of each granule was measured (Fig. 5c). The average size of the major axis was 2.4 μm (±0.8) for the wild-type, while it reached 5.5 μm (±1.7) for *ss3 pii1* and 4.1 μm (±1.0) for *ss4 pii1*. Due to the distorted shape of the *ss3 pii1* starch granules, the identification and measurement of the major axis were difficult. Therefore, the value should be taken as indicative, confirming that this double mutant and the *ss4 pii1* double mutant accumulate starch granules which size is approximately twice larger than that of the wild-type ones.

Leaf starch content and ultrastructure

We determined the leaf starch content in the different genotypes at the end of the light and the dark periods. Four independent cultures were prepared, and for each of them, three independent biological samples were collected. Within an independent culture, all genotypes were cultivated in the same growth chamber under the same conditions and with the same treatment. For each culture, the leaf starch content of the different genotypes was normalized to that of the corresponding wild-type, the average of the three wild-type biological samples being set to 100%. Finally, the mean and the standard error were calculated for each genotype

from 12 samples (four independent cultures × three biological samples; Figs 6, S8).

ss3 behaves as the wild-type since no significant difference in leaf starch content at the end of the day and at the end of the dark period was noticed. The *ss4* mutant accumulated significantly less starch at the end of the day compared with the wild-type but more starch at the end of the night. The *pii1* mutant contained more starch than the wild-type at the end of both periods. No statistically significant difference was detected when *ss3 pii1* was compared with the wild-type or the *ss3* single mutant. The *ss4 pii1* double mutant accumulates significantly less starch than the wild-type and the *ss4* lines at the end of the day (Fig. 6a). However, at the end of the night, the *ss4 pii1* contained in average more starch than the wild-type while the difference between the *ss4* and the *ss4 pii1* was not considered as statistically significant (Fig. 6b).

The amylose content was determined for each genotype after the fractionation of 1.8 mg of purified starch by size exclusion chromatography on Sepharose CL-2B resin. The presence of glucans in each collected fraction was assessed by iodine-spectrophotometry analysis (Fig. 7a). This analysis suggests that *ss3 pii1* starch contains more amylose than the wild-type. Amylopectin- and amylose-containing fractions were pooled independently and the amount of each glucan was determined by enzymatic assay. The starch of the *ss3 pii1* mutant contains 22% amylose while that of the wild-type contains only 15% amylose (Fig. 7b). The amylose content was also estimated using another method that requires the specific precipitation of amylopectin
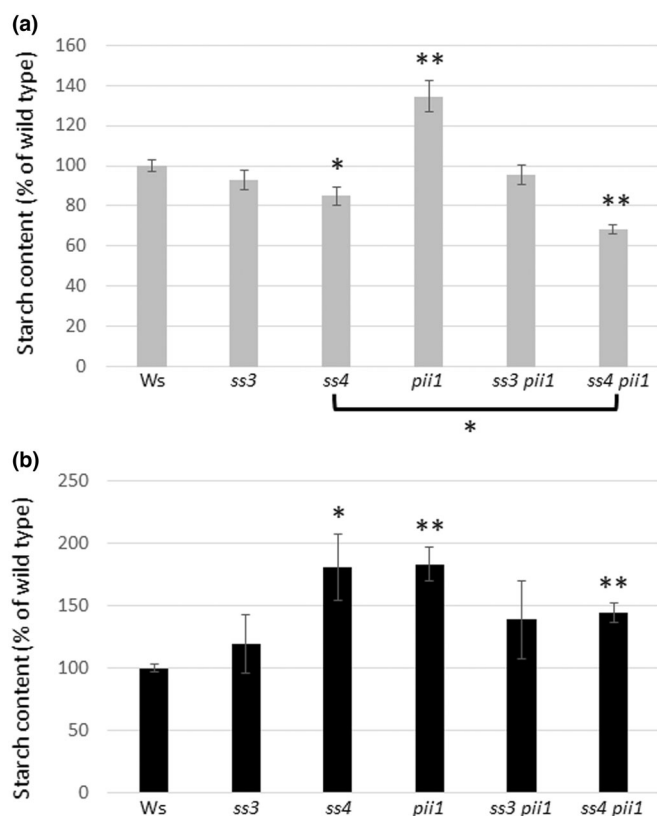
Fig. 6 Starch content. Arabidopsis plants were grown for 3 wk in a growth chamber under 16 h : 8 h, light : dark cycles. Leaves were collected at the end of light (a) or dark phase (b). Four independent cultures were made and each time, three biological samples were harvested. For each culture, the average of wild-type amount was calculated and set at 100%. We then calculate the percentage of wild-type starch amount for the three biological samples of each genotype within the culture. Mean and SE are calculated from the 12 biological samples. Thin vertical bars represent SE. Value obtained for mutant line was compared with the wild-type (and between *ss4* and *ss4 pii1*) using a two-tailed *t*-test (unequal variance). Asterisks indicate statistically significant differences: *, $P < 0.05$; **, $P < 0.001$.

with Concanavalin A. We applied this method on three starch samples prepared from three independent cultures. Here again, the amylose content was increased in the *ss3 pii1* compared with the wild-type being $19.4\% \pm 1.08$ and $6.51\% \pm 0.64$, respectively (Fig. 7c). This increase in amylose content is not associated with a higher content of GBSS1 in starch nor to an increase in ADP-glucose concentration, as these parameters were similar in both *ss3 pii1* and the wild-type lines (Figs S9, S10).

The starch ultrastructure was also characterized by the determination of the amylopectin CLD. 1.8 mg of starch was enzymatically debranched using a mix of isoamylase and pullulanase. The linear glucans were then derivatized by APTS and separated by capillary electrophoresis. After migration, the detection of fluorescence allowed the quantitative determination of the relative proportion of each glucan length. Overall, the profiles of the wild-type and mutant starches were similar (Fig. 8). However, we observed a slight increase in DP 5–10 glucans in the *ss3* mutant, associated with a slight reduction in DP 13–20 glucans, which is in agreement to previously reported results (Zhang *et al.*, 2008).

The profile of the *ss3 pii1* was similar to that of the *ss3*, indicating that PII1 has no function in amylopectin chain elongation. Similarly, the profile of the *ss4 pii1* mutant resembles that of the *ss4* mutant, which is further evidence that PII1 is not involved in determining the final structure of amylopectin.

The crystalline organization of amylopectin molecules was analyzed by XRD. The starch granules from Ws and the double mutants yield similar intensity profiles (Fig. 9). By comparison with the profile of standard potato starch, all specimens correspond to the B-type allomorph, with main characteristic diffraction peaks located at $2\theta = 5.6$, 17.1, 22.2, and $24.1°$. In particular, the peak at $5.6°$ is typical of B-type. It has the highest intensity since the starch granule pellets were X-rayed in excess water, hence in a fully hydrated state. The profile of the *ss4 pii1* starch granules is nearly identical to that of the wild-type, while the peaks of the *ss3 pii1* specimens are somewhat less defined and with a lower intensity, suggesting a slightly lower degree of crystallinity, in line with the higher amylose content of the starch granules. Similar results were observed in the Col-0 genetic background (Fig. S6).

Discussion

Several proteins have already been described as being involved in the control of starch granule initiation in Arabidopsis leaves. However, SS4 is to date the only one with an identified enzymatic activity. *ss4* KO mutants synthesize less than one starch granule per plastid, whereas 5–7 are typically observed in wild-type individuals (Roldán *et al.*, 2007). Moreover, SS4 was shown to control the anisotropic growth of Arabidopsis starch granules by canalizing the deposition of newly synthesized glucans on the equatorial regions, thus explaining their flat and lenticular shape in the wild-type and their spherical shape in the *ss4* mutant (Bürgy *et al.*, 2021). The analysis of the *ss3 ss4* double KO mutant, which is nearly starch-free, highlighted the partial redundancy between SS3 and SS4 in starch initiation suggesting that SS3 is responsible for the priming of the residual starch granules in the *ss4* mutant (Szydlowski *et al.*, 2009). No other enzyme seems capable to compensate for the loss of both SS3 and SS4 to maintain a correct initiation of starch synthesis in Arabidopsis leaves, the very few residual granules being likely the result of stochastic initiation events.

More recently, the PII1 protein was described as mandatory for the correct activity of SS4 (Vandromme *et al.*, 2019). Indeed, PII1 physically interacts with SS4 and in the absence of the former, the number of starch granules produced per plastid significantly drops compared with the wild-type, in a way that resembles that of the *ss4* KO mutant. Therefore, the objective of the present work was to analyze Arabidopsis lines combining mutations of PII1 with those of SS3 or SS4 to better understand the role of these three proteins in the initiation of starch synthesis.

SS4 consistently initiates one starch granule per plastid in the absence of PII1 whatever the status of SS3

As mentioned above, the *pii1* mutant has a reduced number of starch granules in chloroplasts. In most cases, only one starch

Fig. 7 Starch fractionation and amylose content. (a) An amount of starch (1.8 mg), extracted from Arabidopsis leaves, was dispersed in 10 mM NaOH and loaded on a column filled with Sepharose CL-2B matrix. Fraction of 300 μl was collected and analyzed by spectrophotometry using iodine. Black lines correspond to the maximum absorbance of polysaccharide-iodine complex (left axis). Gray lines correspond to the wavelength (λ in nm) at the maximum OD. (b) Polysaccharides were collected and the percentage of amylose was enzymatically determined. Contents of amylose were determined from two starch samples prepared from two different cultures indicated by black triangles and black circles. The vertical bars correspond to the mean of the 2 values. (c) Determination of amylose content using the amylose/amylopectin kit from Megazyme allowing differential precipitation of amylopectin using Concanavalin A. Assay was performed from three starch samples extracted from three different cultures. Vertical bars represent the means and thin bars the SD.
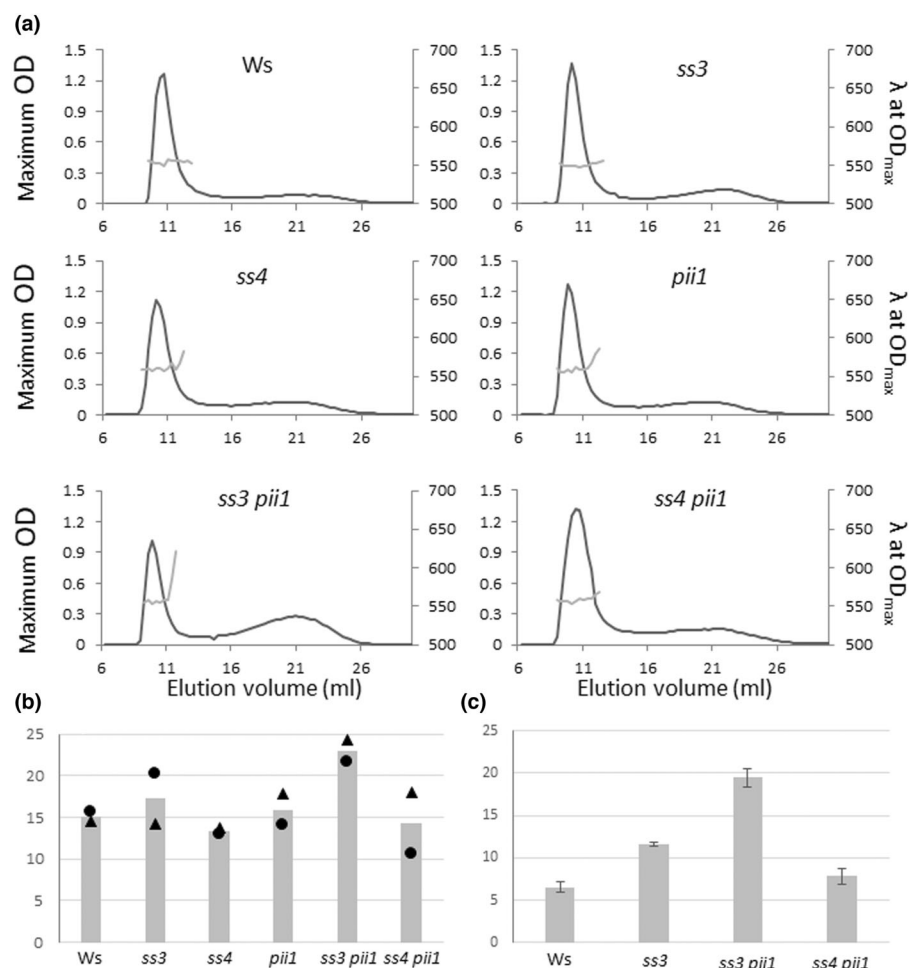
granule can be found in the plastid. However, these granules are larger than those of the wild-type but still have the same flat-lenticular shape. This phenotype suggests that PII1 has a function in controlling the number of starch granules that is distinct from that of SS4. The fact that the shape of the *pii1* mutant granules is identical to that of the wild-type (i.e. lenticular and not round like in the *ss4* mutant) implies that the loss of PII1 does not alter the anisotropic granule growth driven by SS4.

The phenotype of the *pii1* mutant can be explained in two ways. The first explanation is that SS4 is still responsible for the synthesis of, on average, one starch granule per plastid in the absence of PII1, but cannot support the production of the 5–7 starch granules per chloroplast seen in wild-type plants. The second explanation is that, in the absence of PII1, SS4 is no longer able to initiate the starch granule synthesis, this function being then ensured by SS3 only (through a similar or different mechanism and/or partners than that driven by SS4). For that second explanation, one should assume that the N-terminal part of SS4 is still able to control the anisotropic growth of the granules, since these remain flat and lenticular in the *pii1* mutant background.

The analysis of the *ss3 pii1* double mutant allowed testing these two hypotheses. The results revealed that *ss3 pii1* still

produces nearly wild-type amount of starch in the form of one large starch granule per plastid. Since SS3 cannot be responsible for starch initiation in this mutant, this function must still be provided by SS4 in this line. The formation of at least one starch granule per chloroplast, driven by SS4, is very robust since there are almost no starch-free chloroplasts in *pii1* or *ss3 pii1* mutants.

The reason why *ss3 pii1* starch is enriched in amylose is unclear. This could be caused by an increased amount of GBSS responsible for amylose synthesis and/or an increased concentration of ADP-glucose that would stimulate GBSS activity. However, this does not seem to be the case since these parameters are similar in both *ss3 pii1* and wild-type lines (Figs S9, S10). We could only speculate that the increase in the amylose content results from the ability of GBSS to partially compensate for the lack of SS3. It has been demonstrated that SS3 synthesizes the intermediate to long chains of amylopectin (Fontaine *et al.*, 1993; Ral *et al.*, 2006; Fujita *et al.*, 2007; Borén *et al.*, 2008). This capacity can be to a certain extent fulfilled by GBSS1 (Ral *et al.*, 2006), leading to a moderate impact of the SS3 deficiency on amylopectin CLD. Moreover, studies conducted in *Chlamydomonas reinhardtii* revealed that GBSS produces amylose by the extension of and the subsequent cleavage from amylopectin (van de Wal *et al.*, 1998). Consequently, in
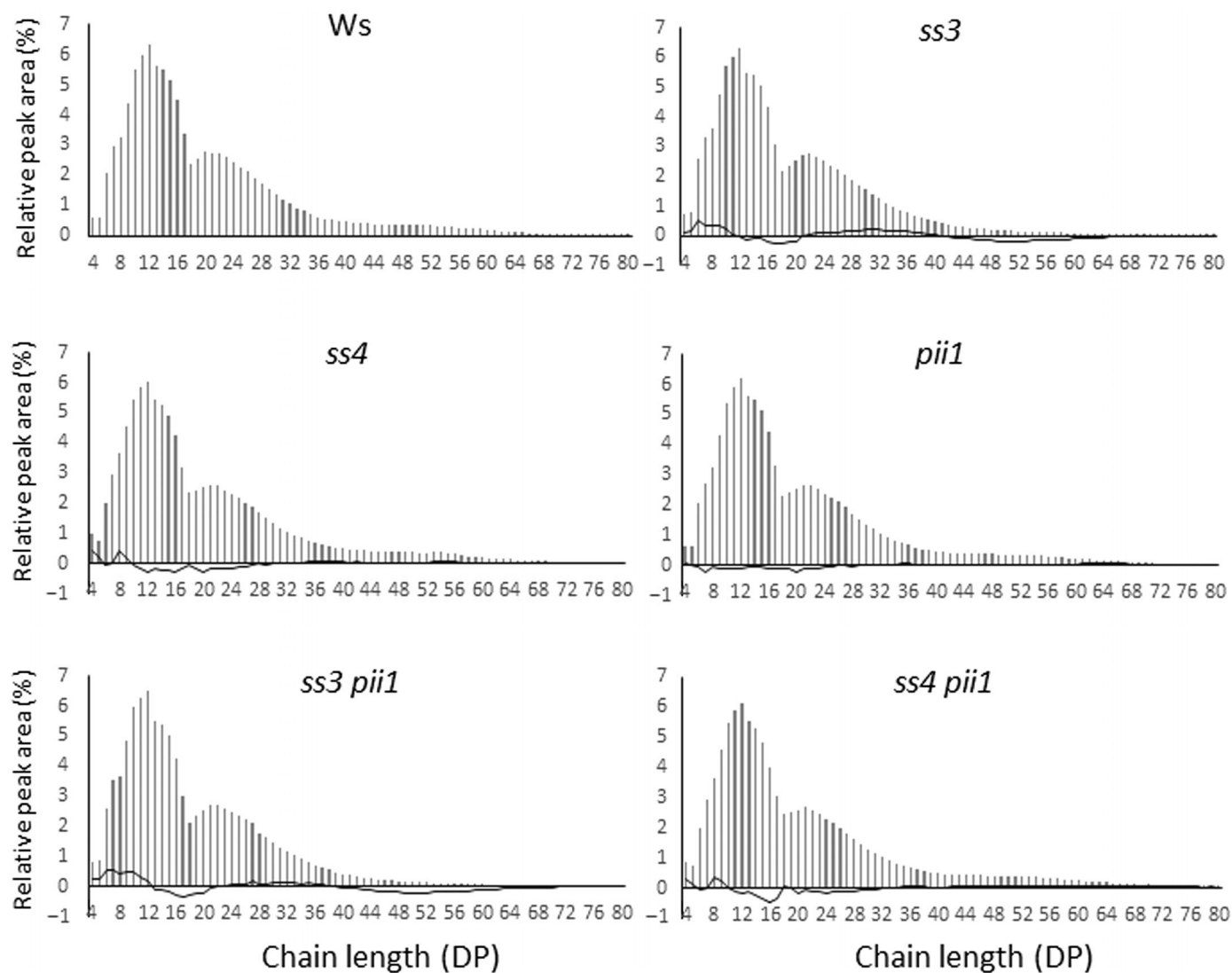
Fig. 8 Amylopectin chain length distribution. An amount of starch (1.8 mg), extracted from Arabidopsis leaves, was debranched using isoamylase and pullulanase. Linear glucans are derivatized with APTS and separated using capillary electrophoresis. Peaks corresponding to DP 4–80 were integrated. Bars represent the mean of relative percentage of each DP obtained from three independent analyses with starch prepared from three independent cultures. Thin black lines correspond to the differential plot between mutant and wild-type profiles.

the absence of SS3, GBSS activity could be partially diverted to synthesizes the very long chains of amylopectin and hence could promote the production of amylose or amylose-like polymers. In fact, the lack of SS3 often induces higher amylose starch as well as modified amylopectin structure and granule shape (Inouchi *et al.*, 1983; Fontaine *et al.*, 1993; Maddelein *et al.*, 1994; Abel *et al.*, 1996; Fujita *et al.*, 2007; Borén *et al.*, 2008). Amylose content is also slightly increased in the Arabidopsis *ss3* mutant (Fig. 7) and (Szydlowski *et al.*, 2011). This effect is exacerbated in *ss3 pii1* probably because of the increased size of the starch granule in that mutant. Indeed, this can amplify the anomaly of the granule shape formation engendered by higher amylose content and altered amylopectin structure. It is therefore possible that the combination of *ss3* with another mutation that greatly reduces the starch granule number per plastid (*mfp1*, *ptst2*, or *ss5* for instance) would lead to the same effect.

SS3 can initiate starch synthesis, a process facilitated by PII1

It was demonstrated that in the absence of SS4, SS3 can prime the synthesis of starch in Arabidopsis leaves (Szydlowski *et al.*, 2009). However, this ability is limited to one starch granule per plastid and not all plastids contain a starch granule. The chloroplasts of cells in the distal region of the leaf (away from the stem) are more likely to produce a starch granule than those in the proximal region (close to the stem) (Vandromme *et al.*, 2019). We investigated whether the SS3-priming aptitude is, mechanically speaking, similar to that of SS4 or if different. To this end and to determine whether SS3-priming ability is affected by PII1, we combined KO mutations for both SS4 and PII1 and we analyzed the phenotype of this double mutant, notably the number of granules per plastid in both the distal and
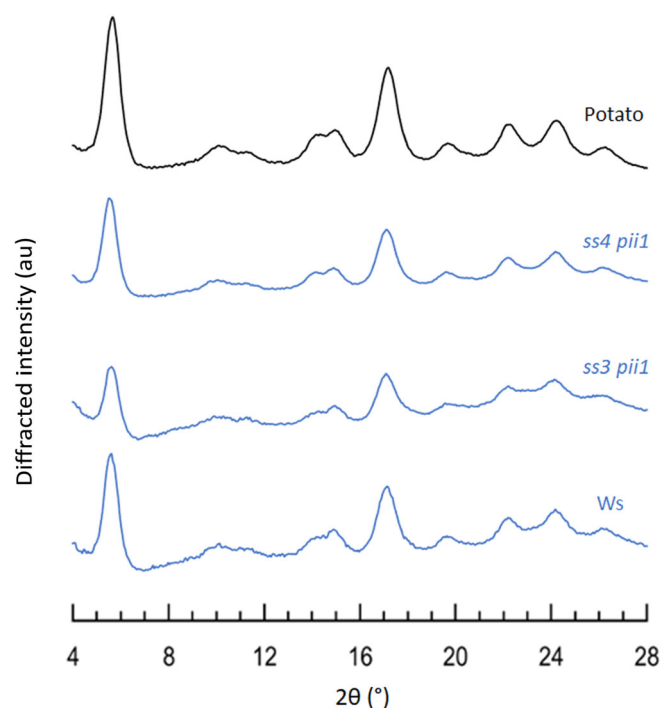
Fig. 9 X-ray diffraction profiles recorded from starch granule pellets in excess water. The contributions of the glass container and the excess water (amount not known with precision) to the scattering have not been subtracted. The profiles recorded from the Arabidopsis Ws specimens have been compared with that of standard potato starch granules prepared in the same conditions. All profiles correspond to a pure B-type allomorph. The intensity has been normalized by calculating the area under each profile between 4 and 28°. au, arbitrary units.

proximal regions of the leaf. We found that the *ss4 pii1* double mutant initiates half as many granules as the single *ss4* mutant whatever the region of the leaf is considered (Fig. 4). Identical result was obtained in both Ws and Col-O genetic backgrounds (Fig. S9). In addition, we also found that *ss4 pii1* accumulates significantly less starch at the end of the day than *ss4*. The fact that the lack of PII1 further reduces the number of granules in an *ss4* mutant background suggests that PII1 facilitates the action of SS3 to sustain the synthesis of the starch granule when SS4 is inactive. It is not known whether this functional interaction arises from a physical interaction between SS3 and PII1 but it has no impact on the interpretation of the results. The study of the physical interaction between SS3 and PII1 as well as of SS3 with the other proteins involved in the process of starch granule initiation (MFP1, SS5, and PTST2) can be the subject of a dedicated complementary work.

The fact that the mechanism of starch granule initiation is similar for both SS3 and SS4 and that it is facilitated by PII1 is not completely surprising if one considers that both starch synthases share common features facilitating interactions with the same protein partners. Indeed, contrary to other canonical starch synthases, SS3 and SS4 share a common chlamydial phylogenetic origin (Ball *et al.*, 2013), and are the only ones that possess two distinct domains of equivalent size with a catalytic GT5-like C-terminal part, and an N-terminal part comprising coiled-coil

domains involved in protein–protein interactions (Abt *et al.*, 2020). This functional overlap is however limited, and in the absence of SS4, a single starch granule is synthesized per chloroplast with a nonnegligible part of starch-free chloroplasts. This overlap of SS3 and SS4 function is not restricted to Arabidopsis since in rice the combined knockdown of SS3a and SS4b leads to a strong alteration of the shape of the starch granules while the corresponding single mutants display wild-type phenotypes (Toyosawa *et al.*, 2016). Arabidopsis genome also codes for a fifth starch synthase (SS5) that can physically interact with PII1 (Abt *et al.*, 2020). Although this protein is closely related to SS4, it is unlikely that it can compensate for the loss of SS4 since it lacks the GT1 domain and is supposed to be catalytically inactive.

Interestingly, the impact of the *ss4* mutation is not homogeneously distributed along the Arabidopsis leaf (Vandromme *et al.*, 2019). Indeed, the average number of starch granules per chloroplast is divided by two in the proximal part of the leaf (0.55 ± 0.06) compared with the distal region (1.03 ± 0.05). We observed the same phenomenon with the *ss4 pii1* double mutant in which the number of starch granules per chloroplast is also divided by approximately two in the proximal region (0.22 ± 0.03) compared with the distal region (0.47 ± 0.03). Since cells and chloroplasts division is greatly reduced in the distal region of the leaf (Gonzalez *et al.*, 2012), proximal and distal regions could be regarded as immature (high cell and plastid division activity) and mature (low cell and plastid division activity) leaves, respectively. Immature leaves of the *ss4* mutant were described as low starch-containing leaves suggesting that starch granule formation is controlled by the status of leaf expansion in a way that is still not understood (Crumpton-Taylor *et al.*, 2013). Our results suggest that PII1 is likely not involved in that control even in the absence of SS4 because the removal of PII1 activity in the *ss4* mutant background does not modify the difference in the chloroplast granule content between distal and proximal regions.

During this study, and by creating and analyzing combinations of mutations, we have demonstrated that, in the absence of PII1, SS4 indeed initiates, almost systematically, the synthesis of one starch granule per chloroplast a number that is similar in *pii1* and *ss3 pii1* (Figs 4, 10). The number of starch granules per plastid is also similar in the wild-type and in *ss3* indicating that when SS4 is present, SS3 does not contribute, or has a minor effect, on starch granule initiation (only a slight difference can be seen in the distal part of *ss3* leaves compared with wild-type). In addition, SS3 can initiate the synthesis of new starch granules, but only if SS4 is absent (i.e. in *ss4* and *ss4 pii1*) and preferentially in cells where the chloroplasts no longer divide (distal part of leaves). Since the phenotype of *ss4 pii1* is more pronounced than that of *ss4*, we could conclude that this mechanism of starch initiation by SS3 is facilitated by PII1 (Fig. 10).

The fact that *pii1* and *ss3 pii1* mutants accumulate one large starch granule per chloroplast and that there are apparently no starch-free chloroplasts in these plants, can be explained in two different ways. First, in the absence of PII1, SS4 can only initiate the synthesis of one starch granule per plastid. It is not clear yet
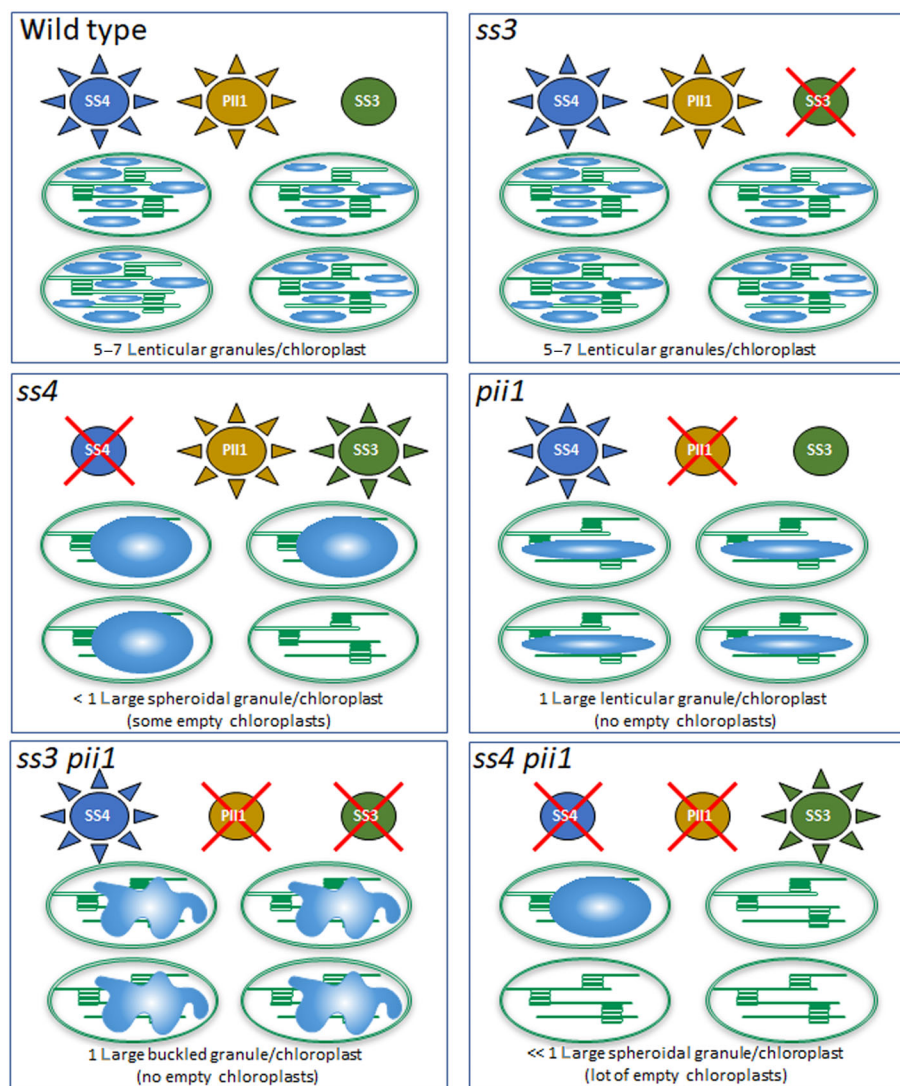
Fig. 10 Summary of the impact of Starch synthase 3 (SS3) and/or SS4 and/or Protein Involved in starch Initiation 1 (PII1) loss on starch granule formation in Arabidopsis chloroplasts. Genotypes are presented at the top of each panel. Starch granules are presented as blue structures inside the chloroplasts. In this schematic view, SS4 is presented as a monomer, and other proteins known to be involved in starch granule initiation are not shown (SS5, MFP1, PTST2). Regarding the number of starch granules per plastid, both the wild-type and the *ss3* mutant have almost the same phenotype as well as *pii1* and *ss3 pii1* (with the exception of granule morphology, which is strongly altered in *ss3 pii1*). When a protein is present in the chloroplast, it is symbolized by a filled circle. If it is involved in the initiation of starch synthesis, then it is represented by a glowing circle. If it is absent, it is crossed out. SS3, SS4, and PII1 are plastidial, but for the clarity of the figure they are represented outside of the chloroplast.

how PII1 could control SS4 activity. The region of SS4 involved in the interaction with PII1 is not clearly defined, but it is likely that, in this hypothesis, PII1 modulates the C-terminal catalytic core region of SS4, which is known to control the initiation of starch. Second, we can speculate that in the absence of PII1, the initiation of starch granules still occurs as in the wild-type plant, but then most, if not all, starch granules merge at the very early stage of their development to finally form a unique large granule in the plastid. This hypothesis is reinforced by the discovery that some starch granule initials coalesce during their growth in Arabidopsis leaves (Bürgy *et al.*, 2021). Thus, in the absence of PII1, coalescence of granule initials would occur at a larger scale compared with the wild-type, leading to the production of a reduced number of larger granules without modification of their morphology since SS4 could still control their anisotropic growth. However, further investigations will be required to discriminate between these two hypotheses and to precisely determine the role of PII1 in the determination of starch granule number per plastid.

Competing interests

None declared.

Author contributions

CV performed and designed experiments. AC, DD and FW participated in experiments. J-LP supervised the electron microscopy observations and performed the XRD analyses. CS performed and interpreted the optical microscopy data. FW and CD'H designed experiments and wrote the manuscript.

ORCID

Adeline Courseaux https://orcid.org/0000-0003-4123-6397
Christophe D'Hulst https://orcid.org/0000-0002-5556-9099
David Dauvillée https://orcid.org/0000-0002-0751-9193
Jean-Luc Putaux https://orcid.org/0000-0002-9760-5369
Corentin Spriet https://orcid.org/0000-0002-5805-3426
Fabrice Wattebled https://orcid.org/0000-0003-0041-8557

Data availability

The data that support the findings of this study are available at doi: 10.5281/zenodo.7780496.

References

Abel GJW, Springer F, Willmitzer L, Kossmann J. 1996. Cloning and functional analysis of a cDNA encoding a novel 139 kDa starch synthase from potato (*Solanum tuberosum* L.). *The Plant Journal* **10**: 981–991.

Abt MR, Pfister B, Sharma M, Eicke S, Bürgy L, Neale I, Seung D, Zeeman SC. 2020. STARCH SYNTHASE5, a noncanonical starch synthase-like protein, promotes starch granule initiation in Arabidopsis. *Plant Cell* **32**: 2543–2565.

Alonso JM, Stepanova AN, Leisse TJ, Kim CJ, Chen H, Shinn P, Stevenson DK, Zimmerman J, Barajas P, Cheuk R et al. 2003. Genome-wide insertional mutagenesis of *Arabidopsis thaliana*. *Science* **301**: 653–657.

Ball SG, Subtil A, Bhattacharya D, Moustafa A, Weber APM, Gehre L, Colleoni C, Arias M-C, Cenci U, Dauvillée D. 2013. Metabolic effectors secreted by bacterial pathogens: essential facilitators of plastid endosymbiosis? *Plant Cell* **25**: 7–21.

Borén M, Glaring MA, Ghebremedhin H, Olsson H, Blennow A, Jansson C. 2008. Molecular and physicochemical characterization of the high-amylose barley mutant Amo1. *Journal of Cereal Science* **47**: 79–89.

Bürgy L, Eicke S, Kopp C, Jenny C, Lu KJ, Escrig S, Meibom A, Zeeman SC. 2021. Coalescence and directed anisotropic growth of starch granule initials in subdomains of *Arabidopsis thaliana* chloroplasts. *Nature Communications* **12**: 6944.

Crumpton-Taylor M, Grandison S, Png KMY, Bushby AJ, Smith AM. 2012. Control of starch granule numbers in Arabidopsis chloroplasts. *Plant Physiology* **158**: 905–916.

Crumpton-Taylor M, Pike M, Lu K-J, Hylton CM, Feil R, Eicke S, Lunn JE, Zeeman SC, Smith AM. 2013. Starch synthase 4 is essential for coordination of starch granule formation with chloroplast division during Arabidopsis leaf expansion. *New Phytologist* **200**: 1064–1075.

Fontaine T, D'Hulst C, Maddelein M, Routier F, Pepin T, Decq A, Wieruszeski J, Delrue B, Van den Koornhuyse N, Bossu J. 1993. Toward an understanding of the biogenesis of the starch granule. Evidence that Chlamydomonas soluble starch synthase II controls the synthesis of intermediate size glucans of amylopectin. *The Journal of Biological Chemistry* **268**: 16223–16230.

Fujita N, Yoshida M, Kondo T, Saito K, Utsumi Y, Tokunaga T, Nishi A, Satoh H, Park J-H, Jane J-L et al. 2007. Characterization of SSIIIa-deficient mutants of rice: the function of SSIIIa and pleiotropic effects by SSIIIa deficiency in the rice endosperm. *Plant Physiology* **144**: 2009–2023.

Gámez-Arjona FM, Raynaud S, Ragel P, Mérida Á. 2014. Starch synthase 4 is located in the thylakoid membrane and interacts with plastoglobule-associated proteins in Arabidopsis. *The Plant Journal* **80**: 305–316.

Gonzalez N, Vanhaeren H, Inzé D. 2012. Leaf size control: complex coordination of cell division and expansion. *Trends in Plant Science* **17**: 332–340.

Guo Q, He Z, Xia X, Qu Y, Zhang Y. 2014. Effects of wheat starch granule size distribution on qualities of Chinese steamed bread and raw white noodles. *Cereal Chemistry Journal* **91**: 623–630.

Helle S, Bray F, Putaux J-L, Verbeke J, Flament S, Rolando C, D'Hulst C, Szydlowski N. 2019. Intra-sample heterogeneity of potato starch reveals fluctuation of starch-binding proteins according to granule morphology. *Plants* **8**: 324.

Inouchi N, Glover DV, Takaya T, Fuwa H. 1983. Development changes in fine structure of starches of several endosperm mutants of maize. *Starch – Stärke* **35**: 371–376.

Jobling S. 2004. Improving starch for food and industrial applications. *Current Opinion in Plant Biology* **7**: 210–218.

Kram AM, Oostergetel GT, van Bruggen E. 1993. Localization of branching enzyme in potato tuber cells with the use of immunoelectron microscopy. *Plant Physiology* **101**: 237–243.

Lu K-J, Pfister B, Jenny C, Eicke S, Zeeman SC. 2018. Distinct functions of STARCH SYNTHASE 4 domains in starch granule formation. *Plant Physiology* **176**: 566–581.

Maddelein M, Libessart N, Bellanger F, Delrue B, D'Hulst C, Van den Koornhuyse N, Fontaine T, Wieruszeski J, Decq A, Ball S. 1994. Toward an understanding of the biogenesis of the starch granule. Determination of granule-bound and soluble starch synthase functions in amylopectin synthesis. *The Journal of Biological Chemistry* **269**: 25150–25157.

Ral J-P, Colleoni C, Wattebled F, Dauvillee D, Nempont C, Deschamps P, Li Z, Morell MK, Chibbar R, Purton S et al. 2006. Circadian clock regulation of starch metabolism establishes GBSSI as a major contributor to amylopectin synthesis in *Chlamydomonas reinhardtii*. *Plant Physiology* **142**: 305–317.

Raynaud S, Ragel P, Rojas T, Mérida Á. 2016. The N-terminal part of *Arabidopsis thaliana* starch synthase 4 determines the localization and activity of the enzyme. *Journal of Biological Chemistry* **291**: 10759–10771.

Roldán I, Wattebled F, Lucas MM, Delvallé D, Planchot V, Jiménez S, Pérez R, Ball S, D'Hulst C, Mérida Á. 2007. The phenotype of soluble starch synthase IV defective mutants of *Arabidopsis thaliana* suggests a novel function of elongation enzymes in the control of starch granule formation. *The Plant Journal* **49**: 492–504.

Schindelin J, Arganda-Carreras I, Frise E, Kaynig V, Longair M, Pietzsch T, Preibisch S, Rueden C, Saalfeld S, Schmid B et al. 2012. Fiji: an open-source platform for biological-image analysis. *Nature Methods* **9**: 676–682.

Seung D, Boudet J, Monroe JD, Schreier TB, David LC, Abt M, Lu K-J, Zanella M, Zeeman SC. 2017. Homologs of PROTEIN TARGETING TO STARCH control starch granule initiation in Arabidopsis leaves. *Plant Cell* **29**: 1657–1677.

Seung D, Schreier TB, Bürgy L, Eicke S, Zeeman SC. 2018. Two plastidial coiled-coil proteins are essential for normal starch granule initiation in Arabidopsis. *Plant Cell* **30**: 1523–1542.

Singh J, Kaur L, McCarthy OJ. 2007. Factors influencing the physico-chemical, morphological, thermal and rheological properties of some chemically modified starches for food applications – a review. *Food Hydrocolloids* **21**: 1–22.

Streb S, Zeeman SC. 2012. Starch metabolism in Arabidopsis. *The Arabidopsis Book* **10**: e0160.

Szydlowski N, Ragel P, Hennen-Bierwagen TA, Planchot V, Myers AM, Mérida A, d'Hulst C, Wattebled F. 2011. Integrated functions among multiple starch synthases determine both amylopectin chain length and branch linkage location in Arabidopsis leaf starch. *Journal of Experimental Botany* **62**: 4547–4559.

Szydlowski N, Ragel P, Raynaud S, Lucas MM, Roldan I, Montero M, Munoz FJ, Ovecka M, Bahaji A, Planchot V et al. 2009. Starch granule initiation in Arabidopsis requires the presence of either class IV or class III starch synthases. *Plant Cell* **21**: 2443–2457.

Tao H, Wang P, Wu F, Jin Z, Xu X. 2016. Particle size distribution of wheat starch granules in relation to baking properties of frozen dough. *Carbohydrate Polymers* **137**: 147–153.

Toyosawa Y, Kawagoe Y, Matsushima R, Crofts N, Ogawa M, Fukuda M, Kumamaru T, Okazaki Y, Kusano M, Saito K *et al.* 2016. Deficiency of starch synthase IIIa and IVb alters starch granule morphology from polyhedral to spherical in rice endosperm. *Plant Physiology* **170**: 1255–1270.

Vandromme C, Spriet C, Dauvillee D, Courseaux A, Putaux JL, Wychowski A, Krzewinski F, Facon M, D'Hulst C, Wattebled F. 2019. PII1: a protein involved in starch initiation that determines granule number and size in Arabidopsis chloroplast. *New Phytologist* **221**: 356–370.

van de Wal M, D'Hulst C, Vincken J-P, Buleon A, Visser R, Ball S. 1998. Amylose is synthesized *in vitro* by extension of and cleavage from amylopectin. *The Journal of Biological Chemistry* **273**: 22232–22240.

Zhang X, Myers AM, James MG. 2005. Mutations affecting starch synthase III in Arabidopsis alter leaf starch structure and increase the rate of starch synthesis. *Plant Physiology* **138**: 663–674.

Zhang X, Szydlowski N, Delvalle D, D'Hulst C, James M, Myers A. 2008. Overlapping functions of the starch synthases SSII and SSIII in amylopectin biosynthesis in Arabidopsis. *BMC Plant Biology* **8**: 96.

Zuiderveld K. 1994. VIII.5. – contrast limited adaptive histogram equalization. In: Heckbert PS, ed. *Graphics gems*. Cambridge, MA, USA: Academic Press, 474–485.

Supporting Information

Additional Supporting Information may be found online in the Supporting Information section at the end of the article.

Fig. S1 Selection of *ss3 pii1* and *ss4 pii1*.

Fig. S2 Plant growth phenotypes (Col-0).

Fig. S3 Starch distribution in leaves as determined by iodin staining (Col-0).

Fig. S4 Images of *ss4* and *ss4 pii1* leaf cells observed by confocal microscopy (Col-0).

Fig. S5 Scanning electron microscopy images of starch granules of the *ss3 pii1* and *ss4 pii1* in the Col-0 background.

Fig. S6 X-ray diffraction profiles of starch extracted from plants of the Col-0 genetic background.

Fig. S7 Distribution of starch granule number per plastid.

Fig. S8 Determination of the average starch content expressed in mg g^{-1} FW ($\pm$SE) as measured in four independent cultures.

Fig. S9 SDS-acrylamide gel electrophoresis of starch-bound proteins.

Fig. S10 ADP-Glucose concentration in Arabidopsis leaves.

Methods S1 Supporting Information Materials and Methods.

Table S1 Information on T-DNA lines and primers used for generation and selection of double mutant lines.

Table S2 Statistical analysis of variations in starch granule number per plastid between genotypes.

Please note: Wiley is not responsible for the content or functionality of any Supporting Information supplied by the authors. Any queries (other than missing material) should be directed to the *New Phytologist* Central Office.